Comparison of techniques for distillation of entanglement over a lossy channel

Caroline Mauron and Timothy C. Ralph
Centre for Quantum Computation and Communication Technology, School of Mathematics and Physics, University of Queensland, St Lucia, Queensland 4072, Australia

(Received 27 July 2022; accepted 8 November 2022; published 5 December 2022)

We analyze three quantum communication protocols that have been proposed in the literature and compare how well they communicate single-rail entanglement. We use specific metrics for output-state purity and probability of success and include the presence of imperfect photon source and detection components. We find that a distributed noiseless linear amplification (NLA) protocol with a relay point placed halfway between Alice and Bob outperforms NLA at Bob's end and a recently proposed purification protocol under most conditions, unless the distance is very small or the photon source component is very good.

DOI: 10.1103/PhysRevA.106.062603

I. INTRODUCTION

The distribution of entangled states is a critical resource in many quantum communication protocols [1–3]. Due to relatively low interaction of quantum states of light with their environment, single-photon entanglement and linear optics produce one of the simplest instances of such protocols [4].

Nevertheless, practical implementation of these schemes has proven highly challenging due to inevitable losses in optical-fiber transmission channels. Methods that were successful in overcoming optical loss for classical communication are unfortunately inadequate in the context of quantum communication. Indeed, it can be shown that deterministic amplification rapidly destroys entanglement, an effect that is not relevant for classical communication [5].

While, historically, most schemes have employed dual-rail encoding [6], interest has recently increased in single-rail encoding [7], where vacuum represents logical zero, and one-photon states represent logical one. In this paper we will focus on the distribution of single-rail entanglement.

Among various techniques that have been proposed to mitigate such loss, noiseless linear amplification (NLA) is an entanglement distillation protocol in which the measurement result heralds whether the amplification was successful or not [8]. It has been used to demonstrate various loss mitigation schemes [9–13]. In particular, this protocol was experimentally demonstrated to be capable of distributing high-fidelity entanglement over loss-equivalent distances of up to 50 km [14] and was subsequently used to implement an error-corrected quantum channel [15]. A similar scheme with photon detection implemented at a central station halfway between Alice and Bob was also demonstrated experimentally [16]. This is a specific example of a general type of repeater protocol based on distributed NLA [17]. While NLA protocols produce entangled states with arbitrarily high, but finite, purity, purification protocols have also been proposed [18,19] as a scheme to obtain perfect entangled-state purity, at the cost of introducing additional source and detection components as well as a decreased probability of protocol success.

A key difficulty in the practical implementation of all such schemes is the efficiency of the single-photon source and detectors used by the protocol [20]. Implementing such components in practice is technologically highly challenging. In recent state-of-the-art experiments, single-photon detection was achieved with 98% efficiency and high time resolution using superconducting nanowire single-photon detectors [21]. Furthermore, single-photon generation was recently demonstrated to yield a 66.7(24)% probability of collecting a single photon using heralded single-photon sources [22,23]. The trade-off between state purity and heralded probability is therefore analyzed here in the presence of these constraints.

We begin by introducing the NLA and our various assumptions in the next section. We illustrate our figures of merit initially by examining direct transmission of single-rail entanglement through a lossy channel. We then see how the situation changes when we introduce our two different NLA protocols. The purification protocol is then introduced in Sec. III, and then we proceed to compare their performances in Sec. IV before briefly concluding in Sec. V.

II. NLA PROTOCOL

We first assume that perfect single-photon sources and single-photon detection devices are available and later relax this assumption in Sec. II D. Environmental noise is modeled as a vacuum state entering the open port of a beam splitter with transmissivity η, such that a photon sent by Alice to Bob either gets transmitted with probability η or gets lost with probability $1-\eta$. A click or "success" is a measurement result that heralds entanglement of the state. In absence of a click, the state is discarded, and another trial is made.

The aim of all protocols analyzed here is that whenever there is a click, Alice and Bob share a state whose entangled component is maximal (unbiased) and which contains as little environmental loss as possible. Such a final state can always be successfully targeted even if there is detection and/or

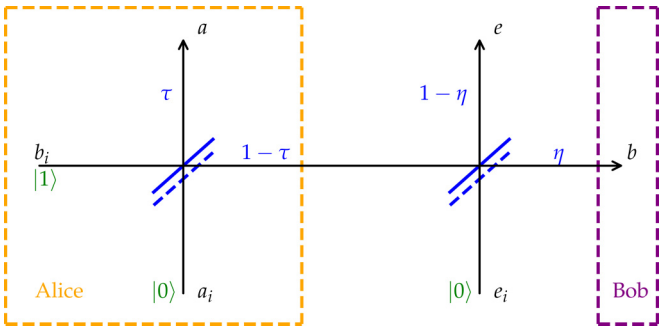

FIG. 1. In the most basic framework, Alice prepares an entangled state using a beam splitter, then sends part of that state over to Bob through a lossy channel of transmissivity η. The channel loss is modeled as a vacuum state $|0\rangle_{e_i}$ entering through the open port of a beam splitter. The parameter τ is chosen such that the resulting output state in modes a and b is a mixture of a pure maximally entangled state $|\psi_f\rangle$ and an environmental loss state $|\psi_0\rangle$. The output-state purity is quantified using the ratio $X = \frac{P_f}{P_0}$.

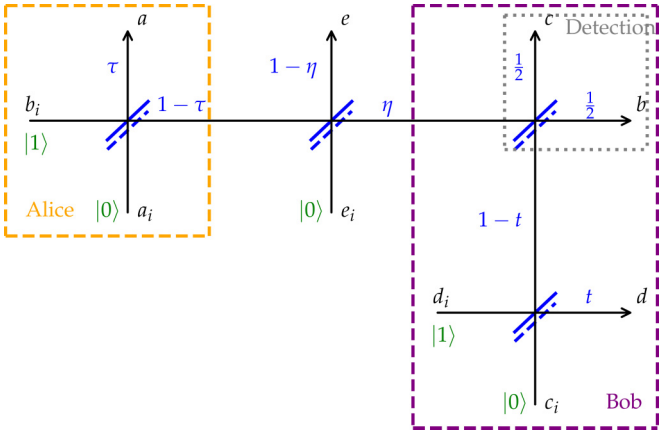

FIG. 2. In the NLA protocol implemented at Bob's end, Alice and Bob each prepare an entangled state by sending a single photon through beam splitters. Alice then sends part of her entangled state to Bob through a channel of transmissivity η. Bob's state and Alice's state are interfered through a 50:50 beam splitter and uses photon detection at output modes b and c. If exactly one photon is detected at mode b or c and no photon is detected at the other mode (representing two possible click states), Alice and Bob will use their respective path-entangled states at outputs a and d.

source loss. We do not consider thermal noise of dark counts here, which could lead to additional error states if included.

A. "Do-nothing" protocol

In order to compare the performance of different protocols, a reference is first established by considering the metrics obtained in the absence of a distillation protocol.

If Alice is in possession of a perfectly pure state with arbitrary entanglement τ and sends this state to Bob through the lossy channel of transmissivity η, as represented in Fig. 1, the output state projected on no environmental losses is

$$|\psi_f\rangle = \sqrt{\tau}|10\rangle_{ab} + \sqrt{1-\tau}\sqrt{\eta}|01\rangle_{ab}, \tag{1}$$

with probability

$$P_f = \tau + \eta(1-\tau), \tag{2}$$

while the projection on environmental losses produces

$$|\psi_0\rangle = \sqrt{1-\tau}\sqrt{1-\eta}|00\rangle_{ab}, \tag{3}$$

with probability

$$P_0 = (1-\tau)(1-\eta). \tag{4}$$

From Eq. (1), the condition of maximal entanglement yields

$$\tau = \frac{\eta}{1+\eta}. \tag{5}$$

We now define the state purity $X = \frac{P_f}{P_0}$, which represents how pure the reduced state $\rho = \mathrm{Tr}_e[|\psi\rangle\langle\psi|]$ is, with $X = \infty$ for a perfectly pure state. The relationship of X to more standard measures of purity such as $\mathrm{Tr}\{\rho^2\}$ is $\mathrm{Tr}\{\rho^2\} = (1+X^2)/(1+X)^2$. For the current case, we find

$$X = \frac{P_f}{P_0} = \frac{2\eta}{1-\eta}. \tag{6}$$

B. NLA at Bob's end

The building block of the NLA protocol as described and implemented in [8,14] is illustrated in Fig. 2. Details of the calculation are given in Sec. A 1.

For the output click state projected on no environmental losses, we obtain

$$|\psi_f\rangle = \sqrt{\tau}\sqrt{1-t}\sqrt{\frac{1}{2}}|10\rangle_{ad} + \sqrt{1-\tau}\sqrt{\eta}\sqrt{\frac{1}{2}}\sqrt{t}|01\rangle_{ad}, \tag{7}$$

with probability

$$P_f = \langle\psi_f|\psi_f\rangle = \tfrac{1}{2}\tau(1-t) + \tfrac{1}{2}(1-\tau)\eta t, \tag{8}$$

and for the output click state projected on environmental losses, we obtain

$$|\psi_0\rangle = \sqrt{1-\tau}\sqrt{1-\eta}\sqrt{1-t}\sqrt{\frac{1}{2}}|00\rangle_{ad}, \tag{9}$$

with probability

$$P_0 = \langle\psi_0|\psi_0\rangle = \tfrac{1}{2}(1-\tau)(1-\eta)(1-t). \tag{10}$$

The condition of maximal entanglement yields

$$\tau = \frac{t\eta}{1-t+t\eta}, \tag{11}$$

so that, after expressing t in terms of η and the state purity X, we find the probability of obtaining a click as

$$P_{\text{success}} = \frac{4\eta(1-\eta)(1+X)}{[2\eta + X(1-\eta)][2+X(1-\eta)]}. \tag{12}$$

More generally, we define P_{success} as the probability that the protocol succeeds, in the sense that the state will not be discarded. This is equal to the click probability in all the protocols analyzed in this paper, other than in the "do-nothing"

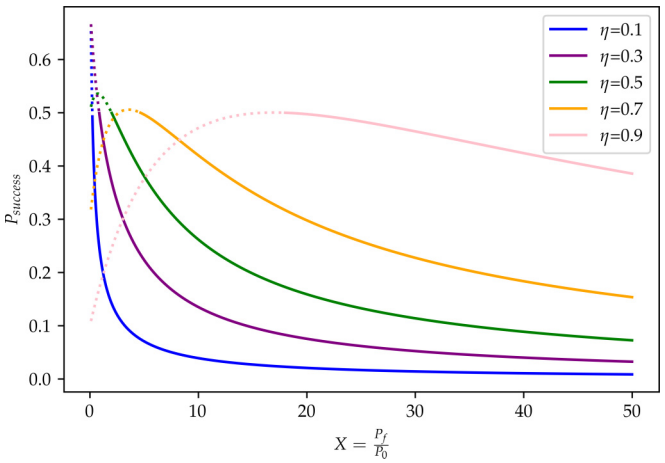

FIG. 3. The probability P_{success} of obtaining a click state is plotted as a function of the state purity X for different channel transmissivities η. The dotted portions of the lines represent areas where a higher X can be obtained from doing nothing, according to Eq. (6). In the solid portions of the lines, the expected trade-off between click probability and state purity is observed, as the odds of obtaining a click decrease for higher purity.

protocol, in which the state is never discarded and therefore $P_{\text{success}} = 1$.

An important benefit of the NLA protocol lies in the fact that, given perfect source and detection components, the purity of the state X can be made arbitrarily high by adjusting the entanglement of Bob's input state. This, however, is expected to come at the expense of a decreased click probability, a relationship illustrated in Fig. 3.

Surprisingly, we find that at small distances (high η, low losses), the click probability can actually increase with X. However, as shown in Sec. A 1, whenever this behavior is observed, the X produced by the NLA protocol is lower than the X obtained without any protocol. Since the probability of success is also lower than 1, applying such a protocol would be worse than doing nothing. In the more typical case (longer distances, $\eta \ll 1$), the expected behavior is observed, and the probability of success decreases as an increasingly purer state is targeted.

C. NLA halfway

An alternative setup as implemented in [16] is now analyzed, with photon detectors placed halfway between Alice and Bob, instead of at Bob's end. This setup is an example of the more general distributed NLA protocol in [17]. The transmissivity of a channel decays exponentially with distance, yielding the conventional assumption [14,24,25] of

$$\eta = e^{-\frac{d}{22}}, \tag{13}$$

where the attenuation loss distance of 22 km is converted from typical optical-fiber loss of 0.2 dB km^{-1}. The transmissivity on each half distance of the channel can therefore be modeled as $\sqrt{\eta}$, such that the total transmissivity over the whole distance is still η.

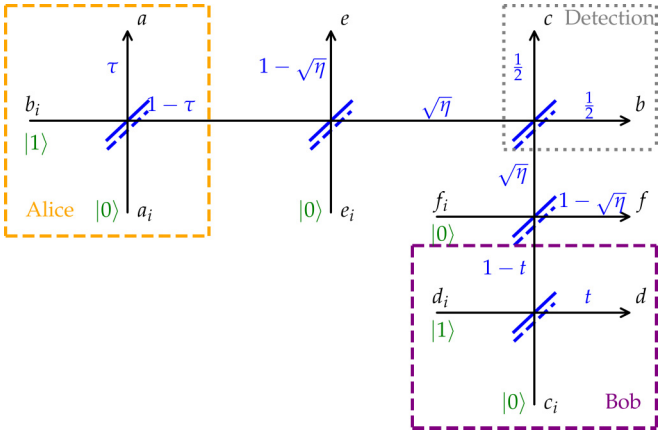

FIG. 4. NLA diagram where the photon detection components b and c have been placed halfway between Alice and Bob. As a result, there are now two environmental loss modes, e and f, each modeled as a vacuum state entering the open port of a beam splitter with transmissivity $\sqrt{\eta}$.

Repeating the calculations for the setup in Fig. 4, the click probability is now

$$P_{\text{success}} = \frac{2\sqrt{\eta}(1-\sqrt{\eta})(1+X)}{[X(\sqrt{\eta}-1)-1]^2} \tag{14}$$

(key intermediary formulas are given in Sec. A 2).

Comparing Eqs. (12) and (14), we obtain the plot displayed in Fig. 5. We see that for a given $X \gg 1$ and assuming $\eta \ll 1$, the click probability in this alternative protocol will now scale with $\sqrt{\eta}$ instead of η, thus leading to a much higher probability of success for a given state purity target.

D. Addition of source and detection noise

We now aim to compare the two setups (NLA at Bob's end and NLA halfway) in the presence of imperfect (i.e., inefficient) photon source and photon detection components. We analyze two situations: (i) perfect sources and imperfect

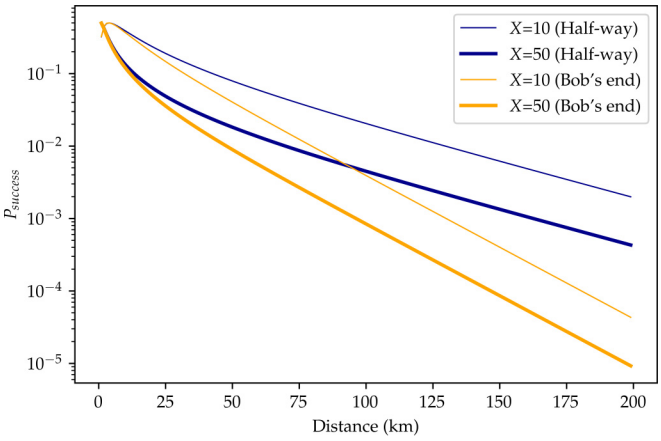

FIG. 5. Comparison of the click probability in NLA protocols done either at Bob's end or halfway between Alice and Bob. At long enough distances, the $\sqrt{\eta}$ scaling will always allow the halfway NLA protocol to outperform, regardless of the state purity chosen.

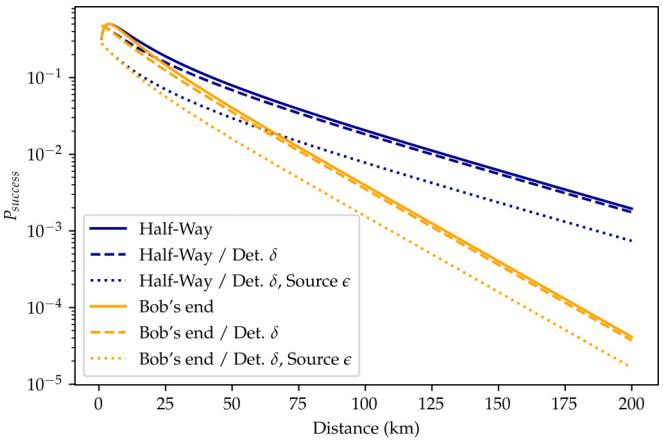

FIG. 6. Comparison of the NLA click probabilities in situations II D and II D, using $\delta = 0.9, \epsilon = 0.9, X = 10$. The improvement brought by implementing photon detection halfway between Alice and Bob is entirely maintained in the presence of imperfect photon source and detection components. However, with a photon source of quality $\epsilon = 0.9$, state purities higher than $X = 18$ cannot be reached.

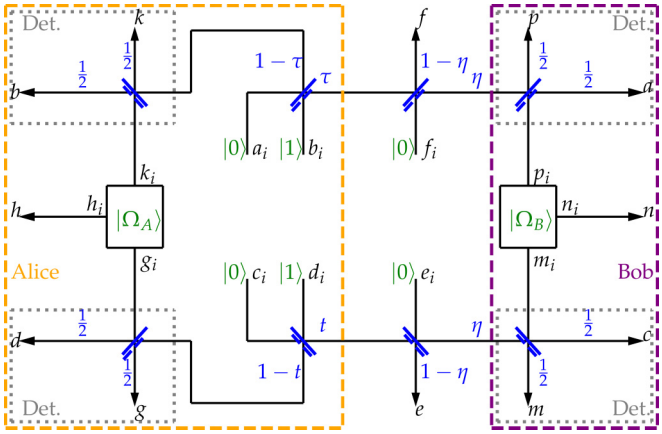

FIG. 7. Purification protocol as proposed in [19]. The resource states $|\Omega_A\rangle$ and $|\Omega_B\rangle$ are prepared such that a single-photon detection at each corner (a "click") heralds complete purity of the output state in modes h and n. In other words, it is guaranteed that no photon was lost to the environment in modes e and f when a click is obtained.

detection (quality δ) and (ii) one imperfect source (quality ϵ) on Bob's end and imperfect detection (quality δ).

In each situation, we compare photon detection at Bob's end to photon detection halfway between Alice and Bob by going through the same calculations as in Sects. II B and II C. Imperfections at the source and the detectors are all modeled as additional environmental loss modes. The resulting diagrams for both situations are available in Appendixes B and C.

Treating situation II D first, we find that in the limit of $X \gg 1$ and $\eta \ll 1$, the probabilities of success are, respectively,

$$P_{\text{success}}^{\text{Bob's end}} \to \frac{4\delta\eta}{X} \tag{15}$$

when the measurement is done at Bob's end and

$$P_{\text{success}}^{\text{Halfway}} \to \frac{2\delta\sqrt{\eta}}{X} \tag{16}$$

when it is done halfway between Alice and Bob. The advantage of putting the detectors halfway between Alice and Bob is therefore maintained with the same order of magnitude, as can be seen in Fig. 6, and we see that the protocol in general is highly resilient to detection noise. If a photon is lost at the heralding detectors, this simply reduces the success probability with limited effect on output quality. (Exact click probability formulas and other intermediary relationships are given in Appendix B.)

Situation II D is unrealistic in the sense that a perfect source would, of course, be used in both places if one was available. However, our aim is to characterize the limitations introduced by the protocol itself, so looking at its performance with an ideal input is useful. The analysis then reveals additional purification constraints introduced by the protocol even if acting on an initially pure state. In this case, it is not possible anymore to reach an arbitrarily high state purity, as the imperfection of the source imposes an upper bound on X. Independently of whether NLA is implemented at Bob's end or halfway, the bound is always given by

$$X_{\max} = \frac{2\epsilon}{1-\epsilon}. \tag{17}$$

In terms of click probabilities, while a lower source quality certainly causes a significant reduction, the relative scaling of $\sqrt{\eta}$ is preserved in favor of the halfway implementation. (Click probabilities and other intermediary formulas are given in Appendix C. The case of on-off detectors was also considered, yielding similar results that are also given in Appendix C.)

III. PURIFICATION PROTOCOL

A. Perfect photon source and detection

We now consider a rather different protocol that we will refer to as the purification protocol. The diagram displayed in Fig. 7 represents the complete purification protocol proposed in [19]. Key differences from the NLA protocols are that Alice now sends two entangled states through the channel (one gets recovered) and uses more complicated resource states:

$$|\Omega_A\rangle = \sqrt{\frac{1}{2}}|001\rangle_{k_i h_i g_i} + \sqrt{\frac{1}{2}}|110\rangle_{k_i h_i g_i},$$
$$|\Omega_B\rangle = \sqrt{\frac{1}{2}}|100\rangle_{m_i n_i p_i} + \sqrt{\frac{1}{2}}|011\rangle_{m_i n_i p_i}. \tag{18}$$

Following the same method as for the NLA protocol, we find that an output state projected on no environmental loss gives

$$|\psi_f\rangle = -\tfrac{1}{8}\sqrt{1-t}\sqrt{\tau}\sqrt{\eta}|10\rangle_{hn} + \tfrac{1}{8}\sqrt{\eta}\sqrt{t}\sqrt{1-\tau}|01\rangle_{hn}, \tag{19}$$

with probability

$$P_f = \tfrac{1}{64}\eta[\tau(1-t) + t(1-\tau)], \tag{20}$$

while the projection on environmental losses yields an empty $|\psi_0\rangle$ and therefore $P_0 = 0$. As a result, the heralded state is absolutely pure ($X = \infty$). In other words, a click means

we know with certainty that no photon was lost to the environment. After setting the usual condition of maximum entanglement ($t = \tau$ here) and considering the 16 possible successful states, we obtain

$$P_{\text{success}} = \tfrac{1}{2}\eta t(1-t). \tag{21}$$

We can set $t = \frac{1}{2}$ to obtain the maximum click probability, and therefore,

$$P_{\text{success}} = \frac{\eta}{8}. \tag{22}$$

B. Imperfect photon source and detection

As in the case of the NLA protocols, the quality of photon sources and detectors must be considered. In line with the earlier assumptions of situation II D in the NLA protocols, we assume that Alice's single-rail entangled states are perfect and consider only the additional noise introduced by the protocol by adding an imperfect source (quality ϵ) to the three branches of each resource state $|\Omega_A\rangle$ and $|\Omega_B\rangle$ and imperfect detection (quality δ) to all eight photon detectors. Repeating the earlier analysis, the state purity is now a constant finite quantity given by

$$X = \frac{2\epsilon^2}{1-\epsilon^2}, \tag{23}$$

and the probability of success is given by

$$P_{\text{success}} = \frac{\delta^4\epsilon^2\eta(1+\epsilon^2)}{4(1+\epsilon)^2} \tag{24}$$

(key intermediary results of this derivation are given in Appendix D). Interestingly, the state purity X produced by this purification protocol can always be reached by the NLA protocols, as $\epsilon \leqslant 1$ guarantees

$$\frac{2\epsilon^2}{1-\epsilon^2} \leqslant \frac{2\epsilon}{1-\epsilon}. \tag{25}$$

IV. PROTOCOL EVALUATION AND COMPARISON

The properties of the different protocols (or absence thereof) are now summarized in Table I, and an example situation is illustrated in Fig. 8 for $d = 25$ km and $\epsilon = 0.99$.

First, it is clear that if $\epsilon < \eta$, doing nothing produces a purer state and a higher P_{success} than any of the protocols considered and is therefore a better choice. The protocols would simply be introducing more noise in the system than there originally was. The scaling of $\sqrt{\eta}$ for NLA halfway vs η for the other two protocols also means that, whatever the other parameters might be, there is always going to be some distance far enough such that this protocol will outperform the others. It also looks likely that the purification protocol may outperform only with very good source quality since both X and P_{success} scale with ϵ^2, instead of ϵ in NLA.

In order to produce a consistent comparison of the three protocols across distances and source quality, a numerical analysis is then performed using the following logic:

(i) If $\epsilon < \eta$, doing nothing is best.

TABLE I. Limiting behavior of the different protocols. The limiting behavior for the click probability P_{success} is obtained under the assumptions $X \gg 1$, $\eta \ll 1$, and $1-\epsilon \ll 1$. The $\sqrt{\eta}$ scaling in P_{success} is critical to the outperformance of halfway NLA vs the other two protocols and ultimately dominates any other effect at long distances, unless the detection and source quality is absolutely perfect.

Source	Protocol	Purity X	P_{success}
Perfect	None	$\frac{2\eta}{1-\eta}$	1
	NLA Bob's end	Arbitrary	$\frac{4\eta}{X}$
	NLA halfway	Arbitrary	$\frac{2\sqrt{\eta}}{X}$
	Purification	∞	$\frac{\eta}{8}$
Quality ϵ	None	$\frac{2\eta}{1-\eta}$	1
	NLA Bob's end	Up to $\frac{2\epsilon}{1-\epsilon}$	$4\delta\eta(\frac{1}{X} - \frac{1-\epsilon}{2})$
	NLA halfway	Up to $\frac{2\epsilon}{1-\epsilon}$	$2\delta\sqrt{\eta}(\frac{1}{X} - \frac{1-\epsilon}{2})$
	Purification	$\frac{2\epsilon^2}{1-\epsilon^2}$	$\frac{\delta^4\epsilon^2\eta}{8}$

(ii) Otherwise, for a given source quality ϵ, the constant purity ratio X obtained in the purification protocol is calculated and fixed at the same level for the two NLA protocols

(iii) The success probability is calculated as a function of distance for all three protocols, and a higher success probability for a given distance is considered to be a superior protocol.

Results of the analysis are displayed in Fig. 9 for $\delta = 0.9$. The halfway NLA protocol appears to be superior in most situations, as the distance scaling dominates. Even in the situations where one of the other protocols is superior, it typically appears to offer only marginal improvements over the halfway NLA protocol. An exception to this rule might be with the advent of future precise source technologies with $\epsilon \approx 1$, whereby operating in the thin green slice in Fig. 9 may result in a significant advantage.

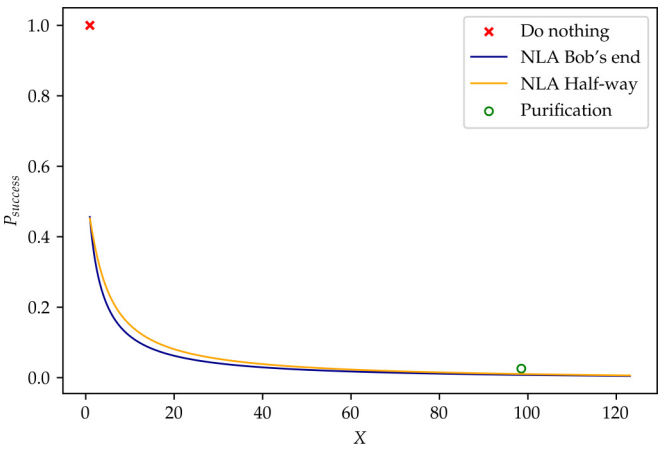

FIG. 8. Click probability P_{success} against state purity X for $d = 25$ km, $\delta = 0.9$, and $\epsilon = 0.99$. The purification protocol is considered to outperform here because its metrics place it above the NLA curve trade-off. If the source quality ϵ is worsened, the green mark moves to the left faster than the NLA curves, such that the halfway NLA soon becomes the best protocol.

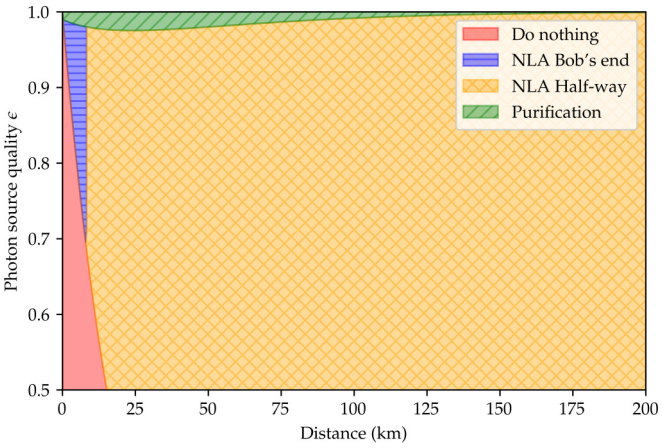

FIG. 9. Best-performing protocol across distances and source quality (detection quality δ is set to 0.9). The halfway NLA protocol offers the best performance in most situations. Exceptions are for very low distances, where doing nothing or NLA at Bob's end may be better, or for very high quality photon source components, where the purification protocol outperforms up to a certain distance.

V. CONCLUSION

We compared the theoretical performance of three quantum communication protocols in terms of output-state purity and probability of success under different assumptions of photon source and detection quality. In most realistic situations, the NLA protocol implemented in a central station between Alice and Bob offers better trade-off metrics than NLA implemented at Bob's end or the purification protocol. This is primarily due to its probability of success scaling with the square root of the channel transmissivity, while the other two protocols are linear. The purification protocol offers the promise of perfect output-state purity, but it is less resilient to source noise than the other protocols due to the higher number of components involved. Building effective quantum communication protocols is an area of active current research, and we expect our results will be of interest in providing a quantitative comparison framework of different schemes. In future work, the analysis may be extended to take into account other experimental considerations such as dark counts and thermal noise, as well as to cover a broader set of protocols.

ACKNOWLEDGMENTS

This research was supported by the Australian Research Council (ARC) under the Centre of Excellence for Quantum Computation and Communication Technology (Grant No. CE170100012). T.C.R. thanks M. Winnel, C. Perez, and S. Slussarenko for motivating discussions.

APPENDIX A: NLA WITH PERFECT PHOTON SOURCE AND DETECTION

1. NLA at Bob's end

We provide full calculations for this first setup where the detections are done at Bob's end and perfect photon source and detection components are available. Intermediary results for the other setups are given without the detailed derivation but follow exactly the same logic.

The input state is

$$|01010\rangle_{a_ib_ic_id_ie_i} = b_i^\dagger d_i^\dagger |00000\rangle_{a_ib_ic_id_ie_i}. \tag{A1}$$

The input operators $b_i^\dagger$ and $d_i^\dagger$ can be written in terms of the output operators based on the diagram from Fig. 2:

$$b_i^\dagger = \sqrt{\tau}a^\dagger + \sqrt{1-\tau}\sqrt{1-\eta}e^\dagger + \sqrt{1-\tau}\sqrt{\eta}\sqrt{\frac{1}{2}}c^\dagger + \sqrt{1-\tau}\sqrt{\eta}\sqrt{\frac{1}{2}}b^\dagger, \tag{A2}$$

$$d_i^\dagger = \sqrt{t}d^\dagger - \sqrt{1-t}\sqrt{\frac{1}{2}}b^\dagger + \sqrt{1-t}\sqrt{\frac{1}{2}}c^\dagger. \tag{A3}$$

Now we can write the input state in terms of the output operators

$$\begin{aligned}|01010\rangle_{a_ib_ic_id_ie_i} = \Big(&\sqrt{\tau}\sqrt{t}a^\dagger d^\dagger - \sqrt{\tau}\sqrt{1-t}\sqrt{\frac{1}{2}}a^\dagger b^\dagger + \sqrt{\tau}\sqrt{1-t}\sqrt{\frac{1}{2}}a^\dagger c^\dagger + \sqrt{1-\tau}\sqrt{1-\eta}\sqrt{t}d^\dagger e^\dagger \\ &- \sqrt{1-\tau}\sqrt{1-\eta}\sqrt{1-t}\sqrt{\frac{1}{2}}b^\dagger e^\dagger + \sqrt{1-\tau}\sqrt{1-\eta}\sqrt{1-t}\sqrt{\frac{1}{2}}c^\dagger e^\dagger + \sqrt{1-\tau}\sqrt{\eta}\sqrt{\frac{1}{2}}\sqrt{t}c^\dagger d^\dagger \\ &- \sqrt{1-\tau}\sqrt{\eta}\sqrt{\frac{1}{2}}\sqrt{1-t}\sqrt{\frac{1}{2}}c^\dagger b^\dagger + \sqrt{1-\tau}\sqrt{\eta}\sqrt{\frac{1}{2}}\sqrt{1-t}\sqrt{\frac{1}{2}}\left(c^\dagger\right)^2 + \sqrt{1-\tau}\sqrt{\eta}\sqrt{\frac{1}{2}}\sqrt{t}b^\dagger d^\dagger \\ &- \sqrt{1-\tau}\sqrt{\eta}\sqrt{\frac{1}{2}}\sqrt{1-t}\sqrt{\frac{1}{2}}\left(b^\dagger\right)^2 + \sqrt{1-\tau}\sqrt{\eta}\sqrt{\frac{1}{2}}\sqrt{1-t}\sqrt{\frac{1}{2}}b^\dagger c^\dagger\Big)|00000\rangle_{a_ib_ic_id_ie_i}.\end{aligned} \tag{A4}$$

After applying the operators to the state, we get

$$\begin{aligned}|01010\rangle_{a_ib_ic_id_ie_i} =&\sqrt{\tau}\sqrt{t}|10010\rangle_{abcde} - \sqrt{\tau}\sqrt{1-t}\sqrt{\frac{1}{2}}|11000\rangle_{abcde} + \sqrt{\tau}\sqrt{1-t}\sqrt{\frac{1}{2}}|10100\rangle_{abcde}\\ &+ \sqrt{1-\tau}\sqrt{1-\eta}\sqrt{t}|00011\rangle_{abcde} - \sqrt{1-\tau}\sqrt{1-\eta}\sqrt{1-t}\sqrt{\frac{1}{2}}|01001\rangle_{abcde}\\ &+ \sqrt{1-\tau}\sqrt{1-\eta}\sqrt{1-t}\sqrt{\frac{1}{2}}|00101\rangle_{abcde} + \sqrt{1-\tau}\sqrt{\eta}\sqrt{\frac{1}{2}}\sqrt{t}|00110\rangle_{abcde}\\ &- \sqrt{1-\tau}\sqrt{\eta}\sqrt{\frac{1}{2}}\sqrt{1-t}\sqrt{\frac{1}{2}}|01100\rangle_{abcde} + \sqrt{1-\tau}\sqrt{\eta}\sqrt{\frac{1}{2}}\sqrt{1-t}\sqrt{\frac{1}{2}}\sqrt{2}|00200\rangle_{abcde}\\ &+ \sqrt{1-\tau}\sqrt{\eta}\sqrt{\frac{1}{2}}\sqrt{t}|01010\rangle_{abcde} - \sqrt{1-\tau}\sqrt{\eta}\sqrt{\frac{1}{2}}\sqrt{1-t}\sqrt{\frac{1}{2}}\sqrt{2}|02000\rangle_{abcde}\\ &+ \sqrt{1-\tau}\sqrt{\eta}\sqrt{\frac{1}{2}}\sqrt{1-t}\sqrt{\frac{1}{2}}|01100\rangle_{abcde}. \end{aligned} \tag{A5}$$

If we project onto ${}_b\langle 0|$ and ${}_c\langle 1|$ (i.e., one of the two click states), most terms drop out, and we get the state

$$|\psi\rangle = \sqrt{\tau}\sqrt{1-t}\sqrt{\frac{1}{2}}|100\rangle_{ade} + \sqrt{1-\tau}\sqrt{1-\eta}\sqrt{1-t}\sqrt{\frac{1}{2}}|001\rangle_{ade} + \sqrt{1-\tau}\sqrt{\eta}\sqrt{\frac{1}{2}}\sqrt{t}|010\rangle_{ade}. \tag{A6}$$

If instead we project onto ${}_b\langle 1|$ and ${}_c\langle 0|$ (the other successful Bell State Measurement (BSM) state), we get

$$|\psi_2\rangle = -\sqrt{\tau}\sqrt{1-t}\sqrt{\frac{1}{2}}|100\rangle_{ade} - \sqrt{1-\tau}\sqrt{1-\eta}\sqrt{1-t}\sqrt{\frac{1}{2}}|001\rangle_{ade} + \sqrt{1-\tau}\sqrt{\eta}\sqrt{\frac{1}{2}}\sqrt{t}|010\rangle_{ade}. \tag{A7}$$

The probabilities of both states are the same since the amplitudes differ by only an experimentally correctable sign change, so the overall probability of success is

$$\begin{aligned}P_{\text{success}} &= 2\langle\psi|\psi\rangle = \tau(1-t) + (1-\tau)(1-\eta)(1-t)\\ &\quad + (1-\tau)\eta t. \end{aligned} \tag{A8}$$

If we want to express the density operator for $|\psi\rangle$ as a mixed state conditional on environment outcome, we can see that projecting $|\psi\rangle$ onto ${}_e\langle 0|$ gives

$$|\psi_f\rangle = \sqrt{\tau}\sqrt{1-t}\sqrt{\frac{1}{2}}|10\rangle_{ad} + \sqrt{1-\tau}\sqrt{\eta}\sqrt{\frac{1}{2}}\sqrt{t}|01\rangle_{ad}, \tag{A9}$$

with probability

$$P_f = \langle\psi_f|\psi_f\rangle = \tfrac{1}{2}\tau(1-t) + \tfrac{1}{2}(1-\tau)\eta t, \tag{A10}$$

and projecting $|\psi\rangle$ onto ${}_e\langle 1|$ gives

$$|\psi_0\rangle = \sqrt{1-\tau}\sqrt{1-\eta}\sqrt{1-t}\sqrt{\frac{1}{2}}|00\rangle_{ad}, \tag{A11}$$

with probability

$$P_0 = \langle\psi_0|\psi_0\rangle = \tfrac{1}{2}(1-\tau)(1-\eta)(1-t). \tag{A12}$$

As expected, we have

$$P_{\text{success}} = 2(P_0 + P_f). \tag{A13}$$

The normalized density operator can be written in the form

$$\hat{\rho} = \frac{P_0\big|\psi_0^{(N)}\big\rangle\big\langle\psi_0^{(N)}\big| + P_f\big|\psi_f^{(N)}\big\rangle\big\langle\psi_f^{(N)}\big|}{P_0 + P_f}, \tag{A14}$$

where $|\psi_0^{(N)}\rangle$ and $|\psi_f^{(N)}\rangle$ are the normalized states, such that

$$\big|\psi_0^{(N)}\big\rangle = |00\rangle_{ad} \tag{A15}$$

and

$$\big|\psi_f^{(N)}\big\rangle = \frac{\sqrt{\tau}\sqrt{1-t}\sqrt{\frac{1}{2}}|10\rangle_{ad} + \sqrt{1-\tau}\sqrt{\eta}\sqrt{\frac{1}{2}}\sqrt{t}|01\rangle_{ad}}{\sqrt{\tau}\sqrt{1-t}\sqrt{\frac{1}{2}} + \sqrt{1-\tau}\sqrt{\eta}\sqrt{\frac{1}{2}}}. \tag{A16}$$

If we want $|\psi_f\rangle$ to be in the maximally entangled state, we need to set τ such that

$$\sqrt{\tau}\sqrt{1-t} = \sqrt{1-\tau}\sqrt{\eta}\sqrt{t}, \tag{A17}$$

so

$$\tau = \frac{t\eta}{1-t+t\eta}. \tag{A18}$$

Now we can replace τ in Eq. (A8), and we get

$$\begin{aligned}P_{\text{success}} &= (1-t)\left(1-\eta+\frac{t\eta^2}{1-t+t\eta}\right)\\ &\quad + \left(1-\frac{t\eta}{1-t+t\eta}\right)\eta t. \end{aligned} \tag{A19}$$

From the expressions for P_0 and P_f, we can also write $X = \frac{P_f}{P_0}$ as a function of t and η, and after some simplifications, we get

$$X = \frac{2t\eta}{(1-\eta)(1-t)}. \tag{A20}$$

Inverting this to get t as a function of X and η, we obtain

$$t = \frac{X(1-\eta)}{2\eta + X(1-\eta)}. \tag{A21}$$

Now we can replace all occurrences of t by their expressions in Eq. (A19), and after some manipulations, we obtain

$$P_{\text{success}} = \frac{4\eta(1-\eta)(1+X)}{[2\eta + X(1-\eta)][2 + X(1-\eta)]}. \tag{A22}$$

For $\eta \ll 1$ and $X \gg 1$, this expression reduces to

$$P_{\text{success}} \approx \frac{4\eta}{X}. \tag{A23}$$

We note the maximum value of P_{success} is reached for an X that satisfies

$$\frac{\partial P_{\text{success}}}{\partial X} = 0, \tag{A24}$$

which gives

$$[2\eta + X(1-\eta)][2 + X(1-\eta)] - (1-\eta)(1+X)[2 + 2\eta + 2X(1-\eta)] = 0. \tag{A25}$$

This is a polynomial of degree 2 in X, and after collecting the terms and solving for the roots, we get

$$X_{\text{root}} = -1 \pm \frac{\sqrt{(\eta+1)(3\eta-1)}}{1-\eta}. \tag{A26}$$

From using $\eta \leqslant 1$, we get $3\eta - 1 \leqslant \eta + 1$, and therefore,

$$X_{\text{root}} \leqslant \frac{2\eta}{1-\eta}, \tag{A27}$$

showing that any X obtained in the left portion of the curve in Fig. 3 (where the probability of success increases with increasing X) is actually always smaller than the X obtained from doing nothing.

2. NLA halfway

Following the same logic as in Sec. A 1, we obtain the following key intermediary results. The click probability is given by

$$P_{\text{success}} = \tau\sqrt{\eta}(1-t) + (1-\tau)(1-\sqrt{\eta})(1-t)\sqrt{\eta} + (1-\tau)\sqrt{\eta}t + (1-\tau)\sqrt{\eta}(1-t)(1-\sqrt{\eta}). \tag{A28}$$

The projection of a click state $|\psi\rangle$ onto no environmental losses gives

$$|\psi_f\rangle = \sqrt{\tau}\sqrt{\sqrt{\eta}}\sqrt{1-t}\sqrt{\frac{1}{2}}|10\rangle_{ad} + \sqrt{1-\tau}\sqrt{\sqrt{\eta}}\sqrt{\frac{1}{2}\sqrt{t}}|01\rangle_{ad}, \tag{A29}$$

with probability

$$P_f = \langle\psi_f|\psi_f\rangle = \tfrac{1}{2}\tau\sqrt{\eta}(1-t) + \tfrac{1}{2}(1-\tau)\sqrt{\eta}t, \tag{A30}$$

while the probability of obtaining a state that includes environmental losses after a click is

$$P_0 = (1-\tau)(1-\sqrt{\eta})(1-t)\sqrt{\eta}. \tag{A31}$$

The condition of a maximally entangled $|\psi_f\rangle$ yields

$$\tau = t. \tag{A32}$$

With this condition, the click probability is given by

$$P_{\text{success}} = 2t\sqrt{\eta}(1-t) + 2(1-t)^2\sqrt{\eta}(1-\sqrt{\eta}). \tag{A33}$$

The ratio X representing state purity is

$$X = \frac{t}{(1-t)(1-\sqrt{\eta})}, \tag{A34}$$

and this can be inverted to obtain t as a function of X, such that

$$t = \frac{X(\sqrt{\eta}-1)}{X(\sqrt{\eta}-1)-1}. \tag{A35}$$

After replacing all occurrences of t by their expressions in Eq. (A33) and some manipulations, we get

$$P_{\text{success}} = \frac{2\sqrt{\eta}(1-\sqrt{\eta})(1+X)}{[X(\sqrt{\eta}-1)-1]^2}. \tag{A36}$$

For $X \gg 1$ and $\eta \ll 1$, this expression reduces to

$$P_{\text{success}} \approx \frac{2\sqrt{\eta}}{X}. \tag{A37}$$

APPENDIX B: NLA WITH IMPERFECT PHOTON DETECTION

1. NLA at Bob's end

Using Fig. 10 and the same logic as in Appendix A, we obtain the following key intermediary results. The click probability is given by

$$P_{\text{success}} = \delta\tau(1-t) + \delta(1-\tau)(1-\eta)(1-t) + \delta(1-\tau)\eta t + 2(1-\tau)(1-t)(1-\delta)\eta\delta. \tag{B1}$$

The projection of a click state $|\psi\rangle$ onto no environmental losses gives

$$P_f = \langle\psi_f|\psi_f\rangle = \tfrac{1}{2}\tau\delta(1-t) + \tfrac{1}{2}(1-\tau)\delta\eta t, \tag{B2}$$

while the probability of obtaining a state that includes environmental losses after a click is

$$P_0 = \delta(1-\tau)(1-t)\big(\tfrac{1}{2}(1-\eta) + \eta(1-\delta)\big). \tag{B3}$$

The condition of a maximally entangled $|\psi_f\rangle$ is unchanged from Sec. A 1,

$$\tau = \frac{t\eta}{1-t+t\eta}. \tag{B4}$$

With this condition, the click probability is given by

$$P_{\text{success}} = \delta(1-t)\left(1-\eta+\frac{t\eta^2}{1-t+t\eta}\right) + \delta\left(1-\frac{t\eta}{1-t+t\eta}\right)\eta t + 2(1-t)(1-\delta)\eta\delta\left(\frac{1-t}{1-t+t\eta}\right). \tag{B5}$$

The ratio X representing state purity is

$$X = \frac{2t\eta}{(1+\eta-2\eta\delta)(1-t)}, \tag{B6}$$

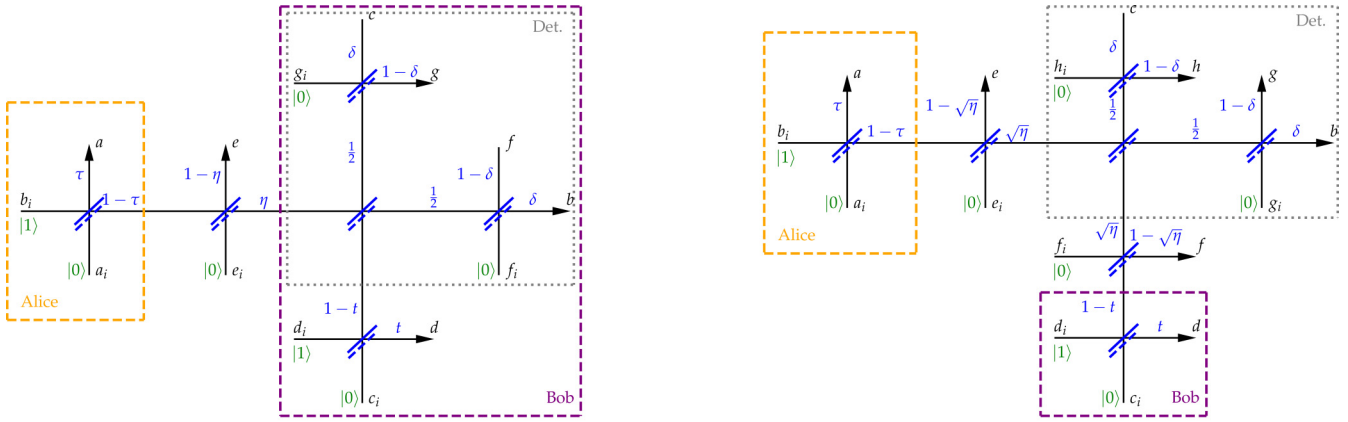

(a) (b)

FIG. 10. NLA protocol in the presence of imperfect detection components for (a) NLA at Bob's end and (b) NLA halfway. Detection noise is modeled as an additional vacuum state entering the open port of a beam splitter of reflection δ, such that a photon going through this component is detected with probability δ and lost with probability $1-\delta$.

and this can be inverted to obtain t as a function of X, such that

$$t = \frac{X(1+\eta-2\eta\delta)}{2\eta + X(1+\eta-2\eta\delta)}. \tag{B7}$$

After replacing all occurrences of t by their expressions in Eq. (B5) and some simplifications, we get

$$P_{\text{success}} = \frac{4\delta\eta(1+\eta-2\eta\delta)(1+X)}{[2\eta + X(1+\eta-2\eta\delta)][2+X(1+\eta-2\eta\delta)]}. \tag{B8}$$

For $\eta \ll 1$ and $X \gg 1$, this expression reduces to

$$P_{\text{success}} \approx \frac{4\delta\eta}{X}. \tag{B9}$$

2. NLA halfway

For this case as represented in Fig. 10, the click probability is

$$P_{\text{success}} = \delta\sqrt{\eta}[(1-\tau)t + \tau(1-t)] + 2\delta\sqrt{\eta}(1-\tau)(1-t)(1-\delta\sqrt{\eta}). \tag{B10}$$

The projection of a click state $|\psi\rangle$ onto no environmental losses gives

$$P_f = \tfrac{1}{2}\sqrt{\eta}\delta[(1-\tau)t + \tau(1-t)], \tag{B11}$$

and projecting onto environmental losses gives

$$P_0 = (1-\tau)(1-t)\delta\sqrt{\eta}(1-\delta\sqrt{\eta}). \tag{B12}$$

The state $|\psi_f\rangle$ can be written in the same way as in Sec. A 2, with only a factor of $\sqrt{\delta}$ in front of it. The condition on τ to reach maximum entanglement is therefore unchanged,

$$\tau = t. \tag{B13}$$

With this condition, the click probability is given by

$$P_{\text{success}} = 2\delta\sqrt{\eta}t(1-t) + 2\delta\sqrt{\eta}(1-t)^2(1-\delta\sqrt{\eta}). \tag{B14}$$

The ratio X representing state purity is given by

$$X = \frac{t}{(1-t)(1-\delta\sqrt{\eta})}, \tag{B15}$$

and this can be inverted to obtain t as a function of X, such that

$$t = \frac{X(1-\delta\sqrt{\eta})}{1+X(1-\delta\sqrt{\eta})}. \tag{B16}$$

After replacing all occurrences of t by their expressions in Eq. (B14) and some simplifications, we get

$$P_{\text{success}} = \frac{2\delta\sqrt{\eta}(1+X)(1-\delta\sqrt{\eta})}{[1+X(1-\delta\sqrt{\eta})]^2}. \tag{B17}$$

For $\eta \ll 1$ and $X \gg 1$, this expression reduces to

$$P_{\text{success}} \approx \frac{2\delta\sqrt{\eta}}{X}. \tag{B18}$$

APPENDIX C: IMPERFECT PHOTON SOURCE AT BOB'S END AND IMPERFECT PHOTON DETECTION

1. NLA at Bob's end

For this case represented in Fig. 11, the click probability is

$$P_{\text{success}} = \epsilon\delta\tau(1-t) + \epsilon\delta(1-\tau)(1-\eta)(1-t) + \epsilon\delta(1-\tau)\eta t + 2\epsilon(1-\tau)(1-t)(1-\delta)\eta\delta + \delta(1-\tau)\eta(1-\epsilon). \tag{C1}$$

The projection of a click state $|\psi\rangle$ onto no environmental losses gives

$$P_f = \tfrac{1}{2}\tau\delta\epsilon(1-t) + \tfrac{1}{2}(1-\tau)\delta\eta t\epsilon, \tag{C2}$$

and projecting onto environmental losses gives

$$P_0 = \delta\epsilon(1-\tau)(1-t)\left(\tfrac{1}{2}(1-\eta) + \eta(1-\delta)\right) + \tfrac{1}{2}(1-\tau)\eta\delta(1-\epsilon). \tag{C3}$$

The state $|\psi_f\rangle$ can be written in the same way as in Sec. A 1, with only a factor of $\sqrt{\delta}\sqrt{\epsilon}$ in front of it. The condition on τ

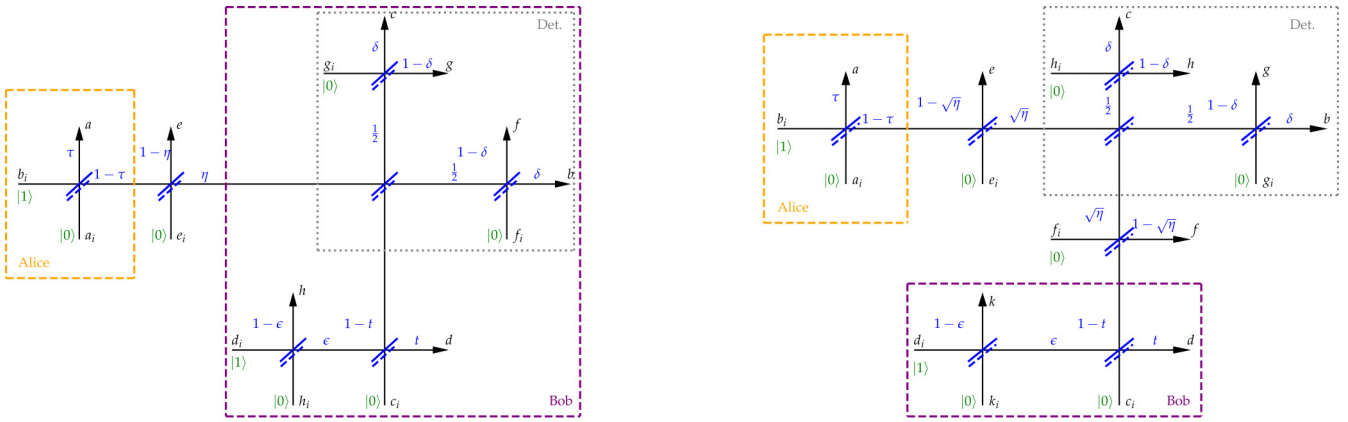

FIG. 11. NLA protocol in the presence of imperfect source and detection components for (a) NLA at Bob's end and (b) NLA halfway. Detection noise is modeled as in the previous case. Source quality is modeled in a similar way, with a probability $1-\epsilon$ for the photon to get lost. We assume Alice has a perfect entangled state in order to focus the analysis on the noise introduced by the protocols.

to reach maximum entanglement is therefore unchanged,

$$\tau = \frac{t\eta}{1-t+t\eta}. \tag{C4}$$

With this condition, the click probability is given by

$$P_{\text{success}} = 2\delta\epsilon\eta\frac{t(1-t)}{1-t+t\eta} + \epsilon\delta(1+\eta-2\eta\delta)\frac{(1-t)^2}{1-t+t\eta} + \eta\delta(1-\epsilon)\frac{1-t}{1-t+t\eta}. \tag{C5}$$

The ratio X representing state purity is given by

$$X = \frac{2t\eta\epsilon}{\epsilon(1+\eta-2\eta\delta)(1-t)+\eta(1-\epsilon)}. \tag{C6}$$

Here, we note that an arbitrarily high X cannot be reached anymore by setting t closer and closer to 1, and the maximum X is given by

$$X_{\max} = \frac{2\epsilon}{1-\epsilon}, \tag{C7}$$

a level at which the click probability is exactly zero. Equation (C6) can still be inverted to obtain t as a function of X, such that

$$t = \frac{X[\epsilon(1+\eta-2\eta\delta)+\eta(1-\epsilon)]}{2\eta\epsilon+X\epsilon(1+\eta-2\eta\delta)}. \tag{C8}$$

After replacing all occurrences of t by their expressions in Eq. (C5) and some simplifications, we get

$$P_{\text{success}} = \frac{2\delta\eta(1+X)(\epsilon+\eta-2\epsilon\eta\delta)[2\epsilon-X(1-\epsilon)]}{[2\eta+X(1+\eta-2\eta\delta)][2\epsilon+X(2\epsilon(1-\eta\delta)+\eta-1)]}. \tag{C9}$$

If we assume $X \gg 1$, $\eta \ll 1$, and $1-\epsilon \ll 1$ (i.e., very good source quality), the expression reduces to

$$P_{\text{success}} \approx 4\delta\eta\left(\frac{1}{X}-\frac{1-\epsilon}{2}\right). \tag{C10}$$

2. NLA halfway

For the case represented in Fig. 11, the click probability is given by

$$P_{\text{success}} = \delta\epsilon\sqrt{\eta}[(1-\tau)t+\tau(1-t)] + 2\delta\epsilon\sqrt{\eta}(1-\tau)(1-t)(1-\delta\sqrt{\eta}) + (1-\tau)\sqrt{\eta}\delta(1-\epsilon). \tag{C11}$$

The projection of a click state $|\psi\rangle$ onto no environmental losses gives

$$P_f = \tfrac{1}{2}\sqrt{\eta}\delta\epsilon[(1-\tau)t+\tau(1-t)], \tag{C12}$$

and projecting onto environmental losses gives

$$P_0 = \epsilon(1-\tau)(1-t)\delta\sqrt{\eta}(1-\delta\sqrt{\eta}) + \tfrac{1}{2}(1-\tau)\delta(1-\epsilon)\sqrt{\eta}. \tag{C13}$$

The state $|\psi_f\rangle$ can be written in the same way as in Sec. A 1, with only a factor of $\sqrt{\delta}\sqrt{\epsilon}$ in front of it. The condition on τ to reach maximum entanglement is therefore unchanged,

$$\tau = t. \tag{C14}$$

With this condition, the click probability is given by

$$P_{\text{success}} = 2\delta\epsilon\sqrt{\eta}t(1-t) + 2\delta\epsilon\sqrt{\eta}(1-t)^2(1-\delta\sqrt{\eta}) + (1-t)\sqrt{\eta}\delta(1-\epsilon). \tag{C15}$$

The ratio X representing state purity is given by

$$X = \frac{\epsilon t}{\epsilon(1-t)(1-\delta\sqrt{\eta})+\frac{1}{2}(1-\epsilon)}. \tag{C16}$$

Similar to the previous case, an arbitrarily high X cannot be reached, and the maximum X is given by

$$X_{\max} = \frac{2\epsilon}{1-\epsilon}, \tag{C17}$$

a level at which the click probability is exactly zero. The formula can still be inverted to obtain t as a function of X,

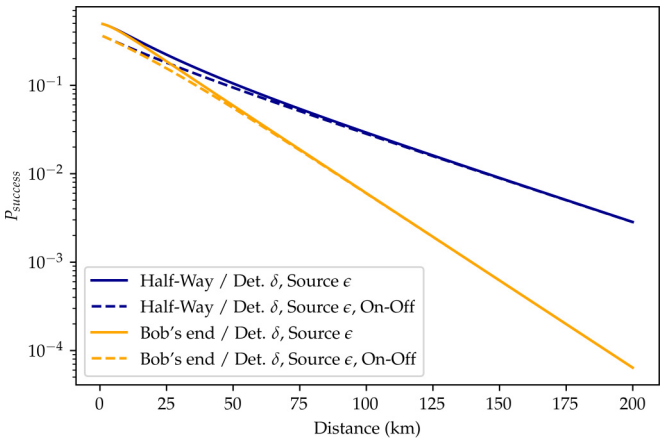

FIG. 12. The probability P_{success} of obtaining a click is plotted against distance for state purity $X = 4$, $\delta = 0.9$, and $\epsilon = 0.9$.

such that

$$t = \frac{X[\epsilon(1-\delta\sqrt{\eta}) + \frac{1}{2}(1-\epsilon)]}{\epsilon + X\epsilon(1-\delta\sqrt{\eta})}. \tag{C18}$$

After replacing all occurrences of t by their expressions in Eq. (C11) and some simplifications, we get

$$P_{\text{success}} = \frac{\delta\sqrt{\eta}(1+X)(1+\epsilon-2\epsilon\delta\sqrt{\eta})[2\epsilon - X(1-\epsilon)]}{2\epsilon[1+X(1-\delta\sqrt{\eta})]^2}. \tag{C19}$$

If we assume $X \gg 1$, $\eta \ll 1$, and $1-\epsilon \ll 1$ (i.e., very good source quality), the expression reduces to

$$P_{\text{success}} \approx 2\delta\sqrt{\eta}\left(\frac{1}{X} - \frac{1-\epsilon}{2}\right). \tag{C20}$$

3. Case of on-off detectors

The case of on-off detectors was also analyzed, still in the presence of detection noise as well as source noise at Bob's end. A click state is now a state where there is at least one photon. Any state with two photons at one detector is then counted as part of ψ_0 together with environmental losses, while ψ_f is the output state projected on no environmental losses and a single photon at each detector.

After repeating the same calculations, for NLA at Bob's end, we find

$$P_{\text{success}} = \frac{2\delta\eta(1+X)(\epsilon+\eta-\delta\epsilon\eta)[2\epsilon - X(1-\epsilon)]}{[2\eta + X(1+\eta-\delta\eta)][2\epsilon+X(2\epsilon-\delta\epsilon\eta+\eta-1)]}, \tag{C21}$$

while for NLA halfway, we find

$$P_{\text{success}} = \frac{2\delta\sqrt{\eta}(1+X)(1+\epsilon-\delta\epsilon\sqrt{\eta})[2\epsilon - X(1-\epsilon)]}{\epsilon[2+X(2-\delta\sqrt{\eta})]^2}. \tag{C22}$$

As displayed in Fig. 12, the improved scaling for NLA halfway is maintained.

APPENDIX D: PURIFICATION PROTOCOL

1. Perfect source and detection

From the diagram in Fig, 7, the input state for the entire system is

$$\begin{aligned}&|010100\rangle_{a_ib_ic_id_ie_if_i} \otimes |\Omega_A\rangle \otimes |\Omega_B\rangle \\ &\quad = b_i^\dagger d_i^\dagger |000000\rangle_{a_ib_ic_id_ie_if_i} \otimes |\Omega_A\rangle \otimes |\Omega_B\rangle,\end{aligned} \tag{D1}$$

with

$$\begin{aligned}|\Omega_A\rangle &= \sqrt{\frac{1}{2}}g_i^\dagger|000\rangle_{k_ih_ig_i} + \sqrt{\frac{1}{2}}k_i^\dagger h_i^\dagger|000\rangle_{k_ih_ig_i}, \\ |\Omega_B\rangle &= \sqrt{\frac{1}{2}}m_i^\dagger|000\rangle_{m_in_ip_i} + \sqrt{\frac{1}{2}}n_i^\dagger p_i^\dagger|000\rangle_{m_in_ip_i}.\end{aligned} \tag{D2}$$

The relevant operators can be written as a function of all the output operators:

$$\begin{aligned}b_i^\dagger &= \sqrt{1-\tau}\sqrt{\frac{1}{2}}b^\dagger + \sqrt{1-\tau}\sqrt{\frac{1}{2}}k^\dagger - \sqrt{\tau}\sqrt{\eta}\sqrt{\frac{1}{2}}a^\dagger \\ &\quad - \sqrt{\tau}\sqrt{\eta}\sqrt{\frac{1}{2}}p^\dagger - \sqrt{\tau}\sqrt{1-\eta}f^\dagger, \\ d_i^\dagger &= \sqrt{1-t}\sqrt{\frac{1}{2}}d^\dagger - \sqrt{1-t}\sqrt{\frac{1}{2}}g^\dagger + \sqrt{t}\sqrt{\eta}\sqrt{\frac{1}{2}}c^\dagger \\ &\quad - \sqrt{t}\sqrt{\eta}\sqrt{\frac{1}{2}}m^\dagger - \sqrt{t}\sqrt{1-\eta}e^\dagger, \\ k_i^\dagger &= -\sqrt{\frac{1}{2}}b^\dagger + \sqrt{\frac{1}{2}}k^\dagger, \\ g_i^\dagger &= \sqrt{\frac{1}{2}}d^\dagger + \sqrt{\frac{1}{2}}g^\dagger, \\ m_i^\dagger &= \sqrt{\frac{1}{2}}c^\dagger + \sqrt{\frac{1}{2}}m^\dagger, \\ p_i^\dagger &= -\sqrt{\frac{1}{2}}a^\dagger + \sqrt{\frac{1}{2}}p^\dagger, \\ h_i^\dagger &= h^\dagger, \\ n_i^\dagger &= n^\dagger.\end{aligned} \tag{D3}$$

After expanding the input state and projecting onto no environment losses (with the help of some computer code), we obtain

$$\begin{aligned}|\psi_f\rangle &= -\tfrac{1}{8}\sqrt{\eta}\sqrt{1-t}\sqrt{\tau}|10\rangle_{hn} + \tfrac{1}{8}\sqrt{\eta}\sqrt{t}\sqrt{1-\tau}|01\rangle_{hn}, \\ P_f &= \tfrac{1}{64}\eta[\tau(1-t) + t(1-\tau)].\end{aligned} \tag{D4}$$

Projecting onto environmental loss states does not yield any term such that $P_0 = 0$. The condition of maximum entanglement yields $\tau = t$, from which we obtained Eq. (22).

2. Imperfect source and detection

Following the same method, we get a click probability of

$$P_{\text{success}} = \tfrac{1}{4}\delta^4\epsilon^2\eta[t(1-\tau) + \tau(1-t)]. \tag{D5}$$

A click state without environmental loss is

$$|\psi_f\rangle = -\tfrac{1}{8}\delta^2\epsilon\sqrt{1-t}\sqrt{\tau}\sqrt{\eta}|10\rangle_{hn} + \tfrac{1}{8}\delta^2\epsilon^2\sqrt{\eta}\sqrt{t}\sqrt{1-\tau}|01\rangle_{hn},$$
$$P_f = \tfrac{1}{64}\delta^4\epsilon^2\eta[\tau(1-t)+\epsilon^2 t(1-\tau)], \tag{D6}$$

and a state with environmental loss $|\psi_0\rangle$ has probability

$$P_0 = \tfrac{1}{64}\delta^4\epsilon^2\eta t(1-\epsilon)(1-\tau)(1+\epsilon) \tag{D7}$$

[and we verify $P_{\text{success}} = 16(P_0 + P_f)$ for 16 successful states]. The condition of max entanglement for $|\psi_f\rangle$ gives

$$\tau = \frac{\epsilon^2 t}{1-t+\epsilon^2 t}. \tag{D8}$$

We can calculate X and P_{success} now with this condition, and we get

$$X = \frac{2\epsilon^2}{1-\epsilon^2}, \qquad P_{\text{success}} = \frac{\delta^4\epsilon^2\eta(1+\epsilon^2)}{4(1+\epsilon)^2}. \tag{D9}$$

If we assume $1-\epsilon \ll 1$, the expression for P_{success} reduces to

$$P_{\text{success}} \approx \frac{\delta^4\epsilon^2\eta}{8}. \tag{D10}$$

[1] A. K. Ekert, Quantum Cryptography Based on Bell's Theorem, Phys. Rev. Lett. **67**, 661 (1991).

[2] N. Gisin and R. Thew, Quantum communication, Nat. Photonics **1**, 165 (2007).

[3] M. A. Nielsen and I. L. Chuang, *Quantum Computation and Quantum Information* (Cambridge University Press, Cambridge, 2000).

[4] T. E. Northup and R. Blatt, Quantum information transfer using photons, Nat. Photonics **8**, 356 (2014).

[5] H.-A. Bachor and T. C. Ralph, *A Guide to Experiments in Quantum Optics*, 3rd ed. (Wiley-VCH, Weinheim, 2019).

[6] E. Knill, R. Laflamme, and G. Milburn, A scheme for efficient quantum computation with linear optics, Nature (London) **409**, 46 (2001).

[7] A. P. Lund and T. C. Ralph, Nondeterministic gates for photonic single-rail quantum logic, Phys. Rev. A **66**, 032307 (2002).

[8] G. Y. Xiang, T. C. Ralph, A. P. Lund, N. Walk, and G. J. Pryde, Heralded noiseless linear amplification and distillation of entanglement, Nat. Photonics **4**, 316 (2010).

[9] S. Kocsis, G. Y. Xiang, T. C. Ralph, and G. J. Pryde, Heralded noiseless amplification of a photon polarization qubit, Nat. Phys. **9**, 23 (2013).

[10] M. Mičuda, I. Straka, M. Miková, M. Dušek, N. J. Cerf, J. Fiurášek, and M. Ježek, Noiseless Loss Suppression in Quantum Optical Communication, Phys. Rev. Lett. **109**, 180503 (2012).

[11] A. E. Ulanov, I. A. Fedorov, A. A. Pushkina, Y. V. Kurochkin, T. C. Ralph, and A. I. Lvovsky, Undoing the effect of loss on quantum entanglement, Nat. Photonics **9**, 764 (2015).

[12] L. Zhou and Y.-B. Sheng, Distilling single-photon entanglement from photon loss and decoherence, J. Opt. Soc. Am. B **30**, 2737 (2013).

[13] L. Zhou and Y.-B. Sheng, Recyclable amplification protocol for the single-photon entangled state, Laser Phys. Lett. **12**, 045203 (2015).

[14] F. Monteiro, E. Verbanis, V. C. Vivoli, A. Martin, N. Gisin, H. Zbinden, and R. T. Thew, Heralded amplification of path entangled quantum states, Quantum Sci. Technol. **2**, 024008 (2017).

[15] S. Slussarenko, M. Weston, L. Shalm, V. Verma, S.-W. Nam, S. Kocsis, T. Ralph, and G. Pryde, Quantum channel correction outperforming direct transmission, Nat. Commun. **13**, 1832 (2022).

[16] P. Caspar, E. Verbanis, E. Oudot, N. Maring, F. Samara, M. Caloz, M. Perrenoud, P. Sekatski, A. Martin, N. Sangouard, H. Zbinden, and R. T. Thew, Heralded Distribution of Single-Photon Path Entanglement, Phys. Rev. Lett. **125**, 110506 (2020).

[17] M. S. Winnel, J. J. Guanzon, N. Hosseinidehaj, and T. C. Ralph, Overcoming the repeaterless bound in continuous-variable quantum communication without quantum memories, arXiv:2105.03586.

[18] C. H. Bennett, G. Brassard, S. Popescu, B. Schumacher, J. A. Smolin, and W. K. Wootters, Purification of Noisy Entanglement and Faithful Teleportation via Noisy Channels, Phys. Rev. Lett. **76**, 722 (1996).

[19] M. S. Winnel, J. J. Guanzon, N. Hosseinidehaj, and T. C. Ralph, Achieving the ultimate end-to-end rates of lossy quantum communication networks, npj Quantum Inf. **8**, 129 (2022).

[20] Y. Ou-Yang, Z.-F. Feng, L. Zhou, and Y.-B. Sheng, Protecting single-photon entanglement with imperfect single-photon source, Quantum Inf. Process. **14**, 635 (2015).

[21] D. V. Reddy, R. R. Nerem, S. W. Nam, R. P. Mirin, and V. B. Verma, Superconducting nanowire single-photon detectors with 98% system detection efficiency at 1550 nm, Optica **7**, 1649 (2020).

[22] F. Kaneda and P. G. Kwiat, High-efficiency single-photon generation via large-scale active time multiplexing, Sci. Adv. **5**, eaaw8586 (2019).

[23] M. M. Weston, H. M. Chrzanowski, S. Wollmann, A. Boston, J. Ho, L. K. Shalm, V. B. Verma, M. S. Allman, S. W. Nam, R. B. Patel, S. Slussarenko, and G. J. Pryde, Efficient and pure femtosecond-pulse-length source of polarization-entangled photons, Opt. Express **24**, 10869 (2016).

[24] C. Panayi, M. Razavi, X. Ma, and N. Lütkenhaus, Memory-assisted measurement-device-independent quantum key distribution, New J. Phys. **16**, 043005 (2014).

[25] S. Khatri, C. T. Matyas, A. U. Siddiqui, and J. P. Dowling, Practical figures of merit and thresholds for entanglement distribution in quantum networks, Phys. Rev. Res. **1**, 023032 (2019).